



HAL
open science

Akt and AMPK activators rescue hyperexcitability in neurons from patients with bipolar disorder

Anouar Khayachi, Malak Abuzgaya, Yumin Liu, Chuan Jiao, Kurt Dejgaard, Lenka Schorova, Anusha Kamesh, Qin He, Yuting Cousineau, Alessia Pietrantonio, et al.

► To cite this version:

Anouar Khayachi, Malak Abuzgaya, Yumin Liu, Chuan Jiao, Kurt Dejgaard, et al.. Akt and AMPK activators rescue hyperexcitability in neurons from patients with bipolar disorder. *EBioMedicine*, 2024, 104, pp.105161. 10.1016/j.ebiom.2024.105161 . inserm-04603069

HAL Id: inserm-04603069

<https://inserm.hal.science/inserm-04603069>

Submitted on 6 Jun 2024

HAL is a multi-disciplinary open access archive for the deposit and dissemination of scientific research documents, whether they are published or not. The documents may come from teaching and research institutions in France or abroad, or from public or private research centers.

L'archive ouverte pluridisciplinaire **HAL**, est destinée au dépôt et à la diffusion de documents scientifiques de niveau recherche, publiés ou non, émanant des établissements d'enseignement et de recherche français ou étrangers, des laboratoires publics ou privés.



Distributed under a Creative Commons Attribution 4.0 International License

Akt and AMPK activators rescue hyperexcitability in neurons from patients with bipolar disorder



Anouar Khayachi,^{a,*} Malak Abuzgaya,^{a,i} Yumin Liu,^{a,i} Chuan Jiao,^b Kurt Dejgaard,^c Lenka Schorova,^d Anusha Kamesh,^a Qin He,^b Yuting Cousineau,^a Alessia Pietrantonio,^a Nargess Farhangdoost,^a Charles-Etienne Castonguay,^a Boris Chaumette,^{b,e,f} Martin Alda,^g Guy A. Rouleau,^{a,h,**} and Austen J. Milnerwood^{a,***}



^aMontreal Neurological Institute, Department of Neurology & Neurosurgery, McGill University, Montréal, Quebec, Canada

^bUniversité Paris Cité, Institute of Psychiatry and Neuroscience of Paris (IPNP), INSERM U1266, Paris, France

^cMcIntyre Institute, Department of Biochemistry, McGill University, Montréal, Quebec, Canada

^dMcGill University Health Center Research Institute, Montréal, Quebec, Canada

^eGHU-Paris Psychiatrie et Neurosciences, Hôpital Sainte Anne, Paris, France

^fDepartment of Psychiatry, McGill University, Montréal, Quebec, Canada

^gDepartment of Psychiatry, Dalhousie University, Halifax, Nova Scotia, Canada

^hDepartment of Human Genetics, McGill University, Montréal, Quebec, Canada

Summary

Background Bipolar disorder (BD) is a multifactorial psychiatric illness affecting ~1% of the global adult population. Lithium (Li), is the most effective mood stabilizer for BD but works only for a subset of patients and its mechanism of action remains largely elusive.

Methods In the present study, we used iPSC-derived neurons from patients with BD who are responsive (LR) or not (LNR) to lithium. Combined electrophysiology, calcium imaging, biochemistry, transcriptomics, and phosphoproteomics were employed to provide mechanistic insights into neuronal hyperactivity in BD, investigate Li's mode of action, and identify alternative treatment strategies.

Findings We show a selective rescue of the neuronal hyperactivity phenotype by Li in LR neurons, correlated with changes to Na⁺ conductance. Whole transcriptome sequencing in BD neurons revealed altered gene expression pathways related to glutamate transmission, alterations in cell signalling and ion transport/channel activity. We found altered Akt signalling as a potential therapeutic effect of Li in LR neurons from patients with BD, and that Akt activation mimics Li effect in LR neurons. Furthermore, the increased neural network activity observed in both LR & LNR neurons from patients with BD were reversed by AMP-activated protein kinase (AMPK) activation.

Interpretation These results suggest potential for new treatment strategies in BD, such as Akt activators in LR cases, and the use of AMPK activators for LNR patients with BD.

Funding Supported by funding from ERA PerMed, Bell Brain Canada Mental Research Program and Brain & Behavior Research Foundation.

Copyright © 2024 The Author(s). Published by Elsevier B.V. This is an open access article under the CC BY-NC-ND license (<http://creativecommons.org/licenses/by-nc-nd/4.0/>).

Keywords: Bipolar disorder; Lithium responsiveness; iPSC-derived neurons; Phosphoproteomics; Akt and AMPK pathways

Introduction

Bipolar Disorder¹ (BD) is a major psychiatric illness affecting 1–3% of the global population.² It is ranked in the top 10 causes of disability and mortality worldwide,

largely due to a 15% suicide rate, in addition to cardiovascular and metabolic comorbidities.^{3–5} Typically, BD has life-long presentation characterized by alternations of mania and depression, often associated with

*Corresponding author.

**Corresponding author.

***Corresponding author.

E-mail addresses: Anouar.khayachi@mcgill.ca (A. Khayachi), Guy.rouleau@mcgill.ca (G.A. Rouleau), Austen.milnerwood@mcgill.ca (A.J. Milnerwood).

ⁱEqual contribution.

Research in context

Evidence before this study

The unknown cause and genetic heterogeneity of BD are major challenges to research efforts, especially those aimed at producing valid disease models in which to explore underlying mechanisms and potential new therapeutics. iPSCs offer a non-invasive opportunity to study neuronal function in cells from individual patients, with known genetic profiles, and associated clinical data e.g., Li responsiveness. Recent reports found hyperexcitability in iPSC-derived neurons from patients with BD, which was selectively reversed by Li in cells from clinically responsive patients. However, the mechanisms underlying neuronal hyperactivity and Li's mode of action remain unclear.

Added value of this study

Our findings replicate neuronal hyperactivity in BD neurons, and selective rescue by Li in BD LR (but not BD LNR) patient neurons, through changes in Na⁺ currents. We found the

potentially therapeutic effect of Li in BD LR neurons was associated with Akt signaling and confirmed that an Akt activator mimics Li effect in BD LR neurones. Further, we found that AMP-activated protein kinase (AMPK) activation reduced the increased neural network activity in neurons from all patients with BD and sodium currents in LNR neurons. This study lays foundations for personalized medicine in BD, and propose alternative treatment strategies to mimic Li's beneficial effects in BD.

Implications of all the available evidence

The capacity to distinguish between BD LR and BD LNR patient's neuronal responses to Li (or other treatments), and thus predict a beneficial clinical response or not, could expedite effective treatment selection for LR patient with BD. AMPK activation may have similarly beneficial effects as Li in all BD patients, regardless of their predicted or actual clinical response to Li.

psychosis and self-harm.¹ Its aetiology is likely multifactorial involving both genetic and environmental factors. Previous studies show BD to be a highly heritable disease (up to 70%), and successful treatment options often work within affected families, suggesting a strong genetic component.^{6–8} Genome Wide Association Studies (GWAS) have revealed many single nucleotide polymorphisms (SNPs) as risk factors for BD, including genes encoding proteins of synaptic, calcium, and second messenger signalling pathways.⁹ Despite these advances, the links between familial presentation, GWAS hits, neurobiological mechanisms, symptoms, and successful treatments, remain unresolved. The unknown cause and genetic heterogeneity of BD are major challenges to research efforts, especially those aimed at producing valid disease models in which to explore underlying mechanisms and potential new therapeutics.

Clinical management is also challenging, due to heterogeneous symptom presentation, phenocopies and similarity to other disorders (e.g., unipolar depression and schizophrenia). Care is further complicated by frequent comorbidity with anxiety or substance abuse among others, that often lead to misdiagnosis and incorrect treatment at early stages. Long-term use of mood stabilizers is the cornerstone of BD clinical management, but clinicians often rely on a “trial-and-error” strategy to find an effective treatment. Consequently, it can take many months or even years to achieve mood stabilization. Despite a low therapeutic index, the mood stabilizer lithium (Li) remains the gold standard treatment for prevention of the illness episodes; it also effectively reduces suicide and overall mortality rates¹⁰ in the ~30% of patients with BD who respond to it. Aside Li, other medications have come from drug repurposing (e.g., anticonvulsants valproate

and lamotrigine), which highlights our poor understanding of BD pathophysiology, and the struggle to develop alternative therapies through mechanistic insights.

To better understand Li as a treatment, and to potentially extrapolate its effects to other compounds with a larger therapeutic index, two major questions remain; i) how is Li effective, and ii) why so for only some patients.^{11,12} Li's mode of action is unknown, with multiple direct and indirect targets and substantial cellular effects.¹³ Li variously affects several kinase/phosphatase cascades e.g., it inhibits protein kinase C (PKC) and glycogen synthase 3b (GSK3b),^{14–17} activates protein kinase B (Akt/PKB), and inhibits inositolpoly-(IMPase) and inositol mono-phosphatase (IMPase).¹³ These molecular changes likely alter several intracellular signalling cascades that modulate neuronal excitability, synaptic transmission, gene expression, and chronobiology. In mouse primary cortical neuron cultures, we previously found long-term Li exposure decreased neuronal sodium (Na⁺) conductance, action potential firing, and calcium (Ca²⁺) flux in individual neurones. Furthermore, Li exposure had effects on the neural network, altering downstream Ca²⁺ signal cascades, decreasing excitatory and increasing inhibitory synapse number and activity.¹⁴

Induced pluripotent stem cell (iPSC) technology facilitates personalised study of neuropsychiatric disorders at the cellular and molecular level, with a non-invasive opportunity to study the function of neuronal cells derived from individual patients. Moreover, data obtained can be aligned with known genetic profiles and associated clinical data e.g., lithium responsiveness. Our previous and others' recent reports^{18,19} found hyperexcitability in iPSC-derived neurons from patients with BD, which was Li selectively reversed in cells from

clinically responsive patients. Li effects were associated with changes to Na⁺ and potassium (K⁺) currents, but the mechanisms underlying neuronal hyperactivity and Li's mode of action were unclear.

Here, we used iPSC-derived forebrain neurons from 5 separate healthy age-matched male individuals (Ctl), 5 separate Li-responsive (LR) patients with BD, and 4 Li-non-responsive (LNR) patients with BD (Table 1). We combined electrophysiology, calcium imaging, biochemistry, transcriptomics, and phosphoproteomics to provide mechanistic insights into neuronal hyperactivity in BD, and Li's mode of action in LR neurons. We aim to guide the search for biomarkers of BD, predictors of Li responsiveness, and potential therapy for LNR patients with BD. We replicated neuronal hyperactivity in BD neurons and selective rescue by Li in BD neurons from LR (and not BD LNR) patients, through changes in Na⁺ currents. Whole transcriptome sequencing revealed altered gene expression in BD neurons in pathways related to glutamatergic synaptic activity, cell signalling and ion transport/channel activity. We found the therapeutic effect of Li in LR neurons was associated with Akt signalling and confirmed that an Akt activator mimics Li effect in LR neurones from patients with BD. Further, we found that AMP-activated protein kinase (AMPK) reduces neural network activity and sodium

currents in LNR neurons. Here, we propose the potential for alternative treatment strategies in BD, such as Akt activators to mimic the therapeutic effect of Li with less risk of toxicity in LR cases, and the use of AMPK activators for LNR patients with BD.

Methods

Research ethics

All cell lines and protocols in the present study were used in accordance with guidelines approved by the institutional human ethics committee guidelines and the Nova Scotia Health Authority Research Ethics Board (REB # 1020604).

iPSC line generation and neuronal differentiation

All the iPSCs were reprogrammed from blood samples of consenting individuals. The iPSCs lines from healthy individual (SBP009, SBP011, SBP012), LR patients with BD (SBP005, 007, 010) and LNR with BD (SBP001, 002, 004) were reprogrammed from lymphocytes as described previously.¹⁹ Other iPSC lines were reprogrammed from peripheral blood mononuclear cells (PBMCs) using CytoTune iPSC Sendai reprogramming kit (Thermo Fisher Scientific) according to the manufacturer's protocol with the adequate quality control criteria for iPSC validation. 9 out of the total of 14 iPSCs lines (3 of 5 per group) overlap with previous studies^{19,20} with additional newly reprogrammed lines for this study.

iPSCs were cultured on a Matrigel (Corning) coated plate with mTeSR 1 medium (STEMCELL Technologies) and neural progenitor cells (NPCs) induction was performed according to Stem cell Technologies protocol with STEMdiff™ SMADi Neural Induction kit (STEMCELL Technologies). On Day 0, a single-cell suspension of iPSC was generated using Gentle Cell Dissociation reagent and 10,000 cells per microwell was seeded in an ultralow attachment 96-well plate to generate Embryoid bodies (EBs), cultured in STEMdiff™ Neural Induction Medium + SMADi + 10 μM Y-27632. From Day 1 to Day 4, a daily partial (3/4) medium change was performed using STEMdiff™ Neural Induction Medium + SMADi. On Day 5, EBs were harvested using a wild-board 1 ml serological pipettes and 40 μm strainer and transferred to a single well of a 6-well plate coated with Poly-L-ornithine hydrobromide (PLO) and laminin before. A daily full medium change was performed from Day 6 to Day 11. After the neural induction efficiency was determined higher than 75%, Neural rosettes are manually selected using STEMdiff™ Neural Rosette Selection Reagent on Day 12 and replated onto a single well of PLO/Laminin coated 6-well plate. With continuous daily full medium change, selected rosette-containing clusters attached, and NPC outgrowths formed a monolayer between the clusters. Neural Progenitor Cells (NPCs) were ready for passage 1

Ctl					
Sample	Affected	Ethnicity	Sex	Age	Li response
SBP009	n/a	Caucasian	M	51	n/a
SBP011	n/a	Caucasian	M	61	n/a
SBP012	n/a	Caucasian	M	53	n/a
3448	n/a	Caucasian	M	50	n/a
L2131	n/a	Caucasian	M	53	n/a
BD LR					
Sample	Affected	Ethnicity	Sex	Age	Li response
4119	BDI	Caucasian	M	54	9/10
4146	BDI	Caucasian	M	40	9/10
SBP005	BDI	Caucasian	M	41	10/10
SBP007	BDI	Caucasian	M	34	9/10
SBP010	BDI	Caucasian	M	50	9/10
BD LNR					
Sample	Affected	Ethnicity	Sex	Age	Li response
SBP001	BDI	Caucasian	M	51	3/10
SBP002	BDI	Caucasian	M	58	1/10
SBP004	BDI	Caucasian	M	40	0/10
4120	BDI	Caucasian	M	55	0/10

Sample ID: all samples are sourced from blood SBP001, 2, 4, 5, 7, 9, 10, 11, 12 (iPSC are derived from lymphocytes) and 3448, L2131, 4119, 4146, 4120 (iPSC are derived from peripheral blood mononuclear cells); n/a, not applicable; BDI, Bipolar Disorder type I; M, Male; Age, years; Li response as rated by clinical assessment with the standardized Alda scale.

Table 1: Origin of patient samples from patients with BD, clinical response to Li treatment, and matched controls.

when cultures are approximately 80–90% confluent (typically at Day 17 to Day 19). NPCs were maintained using STEMdiff™ Neural Progenitor Medium and ready to differentiate after two passages with Cell Gentle Dissociate Reagent. For the final differentiation into Hippocampal neurons, NPCs were digested with Accutase and then differentiated onto PLO/laminin coated plates/coverslips with final differentiation media which is BrainPhys media (STEMCELL Technologies) supplemented with Glutamax (Fisher), N2, B27, 200 nM ascorbic acid (STEMCELL Technologies), 500 µg/ml cyclic AMP (SIGMA), 20 ng/ml brain-derived neurotrophic factor (BDNF, GIBCO), 10 ng/ml Wnt3a (R&D Systems), and 1 µg/ml laminin for 2 weeks; with a medium change of 3 times per week. After 2 weeks of differentiation, final differentiation media is replaced by STEMdiff™ forebrain Neuron Maturation kit until neurons are used. Maturation media were changed twice a week.

Immunocytochemistry and confocal imaging

iPSC-derived neurons were fixed in phosphate-buffered saline (PBS) containing 3.7% formaldehyde and 5% sucrose for 1 h at room temperature (RT), then in NH₄Cl (50 mM) for 10 min. Neurons were then permeabilized for 20 min in PBS containing 0.1% Triton X-100 and 10% goat serum (GS) at RT and immunostained with a guinea-pig polyclonal anti-vGluT1 (1/4000; Millipore AB5905, RRID: AB_2301751), a mouse monoclonal anti-BIII tubulin (1/1000; Sigma T8660), a mouse anti-Sox 2 (1/500 Abcam ab79351, RRID: AB_10710406), a rabbit anti-Nestin (1/600 Sigma N5413, RRID: AB_1841032) and DAPI (1/5000 Sigma D9542), antibodies in PBS containing 0.05% Triton X-100 and 5% GS. Cells were washed three times in PBS and incubated with the appropriate secondary antibodies (1/1000) conjugated to Alexa 555 or Alexa 488 and mounted with Prolong (ThermoFisher P36930) until confocal examination.

The images (1024 × 1024) were acquired with a ×20 lens (numerical aperture NA 1.4) on an SP8 confocal microscope (Leica Microsystems). Z-series of 6 images of randomly selected field were compressed in 2D using the max projection function in image j (FIJI).

Electrophysiological recordings and analyses

All electrophysiological signals were acquired using Multiclamp 700B amplifier digitized at 10 kHz and pClamp 10 software. Data were analyzed in Clampfit 10 (Molecular Devices).

External and internal solutions

iPSC-derived neurons on coverslips were transferred to a recording chamber in a recording buffer containing (in mM): 167 NaCl, 10 D-glucose, 10 HEPES, 2.4 KCl, 1 MgCl₂, and 2 CaCl₂ (300–310 mOsm, pH adjusted to 7.4 with NaOH) supplemented by SC79 (5µM, Tocris 4635)

or A769662 (1µM, Sigma SML2578) depending on the experimental condition. Whole cell patch clamp experiments were carried out at 25–27 °C.

For all recordings, pipettes were filled with a potassium-based solution containing (in mM): 145 K-gluconate, 3 NaCl, 1 MgCl₂, 1 EGTA, 0.3 CaCl₂, 2 Na-ATP, 0.3 Na-GTP, 0.2 cAMP and 10 HEPES (290 mOsm, pH adjusted to 7.3 with KOH). Patch pipettes displayed a resistance of 4–7 MΩ.

Synaptic events recordings

sEPSCs and sIPSCs were recorded in voltage clamp mode, holding cells at –55 and 0 mV respectively. Synaptic events were sampled for 5 min and then exported to Clampfit 10.7 software with which the amplitude and frequency of synaptic events were quantified (threshold 10 pA); all events were checked by eye and monophasic events were used for amplitude and decay kinetics, while others were suppressed but included in frequency counts as in these studies.^{21,22} Tolerance for series resistance (Rs) was <30 MΩ and uncompensated; ΔRs tolerance cut-off was <20%.

Sodium and potassium currents

Sodium and potassium currents were acquired in voltage-clamp mode. Sodium channel currents are reported as inward peak currents and potassium channel currents as outward currents during series of voltage steps of 10 mV from –70mV to 20 mV. Currents were directly normalized by the cell capacitance during recordings in pClamp 10 software.

Neuronal excitability

for assessing neuronal excitability, action potential (AP) firing was recorded in current-clamp mode in response to incremental, hyperpolarizing followed by depolarizing current injections of 1s duration (3 pA increment of 15 steps). The number of AP firing was plotted to the corresponding current steps using Clampfit 10.7 software. In current-clamp mode, the resting membrane potential of all cells was adjusted to ~ –65 mV by injection of a small negative current if needed.

RNA extraction and RNA sequencing

RNA sequencing was performed on bulk cultures of neurons at ~ 30 days post-differentiation treated or not with Li for 7 days in 5 Ctl, 5 LR and 4 LNR patient lines with BD (28 samples). Total RNA was extracted from ~3×10⁶ cells for each condition using miRNeasy kit (Qiagen, USA) according to the manufacturer's instructions. RNA was resuspended in RNase-free water. The RNA concentration was measured on the Synergy H4 microplate reader. RNA was sent to Genome Quebec center for sequencing. Library preparation was done using the TruSeq Stranded Total RNA Kit (Illumina) with Ribo-Zero depletion. Sequencing was done

on the NovaSeq 6000 at 150bp paired end reads with a total of 113M reads (~17Gb/sample).

Differential expression analysis, deconvolution, clustering, and pathway enrichment

The count alignment and quantification were performed with STAR (v2.7.3a)²³ and RSEM (v1.3.1).²⁴ The reference genome used was GRCh38. p13. The quantified raw counts were transformed to log2CPM with edgeR package (version 3.14.0).²⁵ Genes with at least one count per million (CPM) in more than 25% samples were retained. Samples having connectivity with other samples were retained (Z-scored standard deviation < 3.5). Cluster samples analysis was performed using flashClust (v1.01) and colored by sample information with WGCNA (v1.72).²⁶ Limma (version 3.56.0)²⁷ was used for differential expression analysis. We separately compared gene expression levels between Ctl and BD lines. In a second analysis, we compared the different effect of Lithium in BD LR and BD LNR with the following design matrix in Limma (LR-Li vs. LR + Li)–(LNR-Li vs. LNR + Li). The hidden confounders were detected by surrogate variable analysis (SVA v3.50).²⁸ Significant genes (FDR-corrected p value < 0.05), $|\log_{2}FC| > 1$) were further enriched with GO pathways (clusterProfiler R package 4.8.1).²⁹ For the enrichment pathways, we used adjusted p value < 0.05 as threshold to define significant enriched pathways, which was corrected for multiple testing using FDR. Supervised cell-type deconvolution was performed based on the pipeline described by Sutton et al.³⁰

Phosphoenrichment and phosphoproteomic analysis

Protein lysis and digestion

~30 days post-differentiation iPSC-derived neurons were collected in 50 μ L of Tris-buffer saline (TBS) solution supplemented with protease inhibitor cocktail (Sigma P8340) and phosphatase inhibitors (PhosSTOP, Sigma 4906845001). ~3 \times 10⁶ cells per condition (~1.2 mg of proteins). For each sample (n = 4 per group), 50 μ L of cell pellets were lysed, reduced, and alkylated in lysis buffer (8 M Urea, 2 mM DTT, 100 μ M Orthovanadate, supplemented with 10 mM iodoacetamide (IAA) after half an hour). The samples were then diluted in 50 mM ammonium bicarbonate to a Urea concentration of 1 M. Proteins were digested overnight at 25 °C with trypsin (Promega) with an enzyme/substrate ratio of 1:250. After digestion, samples were supplemented with 2 volumes of acetonitrile (ACN) and precipitate (DNA/RNA) was eliminated after a 10 min centrifugation in an Eppendorf centrifuge at 14,000 rpm.

TiO₂ phosphoenrichment

The supernatant was supplemented with 6% Trifluoroacetic acid (TFA) and transferred to Eppendorf

tubes containing 10 μ L of 5 μ m TiO₂ beads (Canadian Biosciences) and incubated for 30 min on a rotating wheel. The supernatant was aspirated and the TiO₂ beads were washed twice with 50% ACN/0.5% TFA in 200 mM NaCl and once with 50% ACN/0.1% formic acid (FA). Phosphopeptides were eluted with 10% ammonia in 50% ACN. Samples were dried down in a speed vac, resuspended in 20 μ L of 0.1% FA in water and stored frozen, if not processed immediately.

Mass spectrometry: RP-nanoLC-MS/MS

Mass spectrometry data were acquired using an UHPLC Easy nLC 1000 (Thermo Scientific) coupled to an Orbitrap Q Exactive HF mass spectrometer (Thermo Scientific). 50% of the phosphopeptide enriched samples were first trapped (Acclaim PepMap 100C18, 3 μ m, 2 cm) before being separated on an analytical column (Acclaim, C18 2 μ m, 25 cm). Trapping was performed in solvent A (0.1% FA in water), and the gradient was as follows: 2–20% solvent B (0.1% FA in 90% ACN, 10% water) in 90 min, 20–38% in 60 min, 38–90% in 10 min, maintained at 90% for 10 min, then, back to 0% solvent B in 10 min. The mass spectrometer was operated in data-dependent mode. Full-scan MS spectra from m/z 375–1500 were acquired at a resolution of 120,000 at m/z 400 after accumulation to a target value of 5×10^6 . Up to 25 most intense precursor ions were selected for fragmentation. HCD fragmentation was performed at normalized collision energy of 35% after the accumulation to a target value of 1×10^5 . MS/MS was acquired at a resolution of 30,000. A dynamic exclusion was set at 6 s.

Bioinformatics and databases for protein identification (BioID) and analysis

All MS/MS raw data files were converted into peak lists using Mascot Peak Distiller (Matrix Science). Mgf files were searched against the curated human proteome database (UniProt: *Homo sapiens*) using the Mascot search engine (Matrix Science) with the following parameters: enzyme: trypsin. Missed cleavages: 1. #C13:1. Fixed modifications: C-acetamidation. Variable modifications: oxM and phospho-T and phospho-S. Precursor mass accuracy: 6 ppm. MSMS mass accuracy: 50 ppm. Instrument type: ICRFT. Mascot files were imported into Scaffold v5 (Proteome Software Inc), and a second search engine (X!Tandem) was requested to search the data again, after which the combined data was validated through the trans proteomic pipeline. Data were visualized as TSCs in scaffold v5 software, counting only the phosphopeptides identified with protein threshold of 20%, Min # peptides of 1 and peptide threshold of 95% and batched in categories according to patient and experimental parameters (Ctl, BD LR, BD LNR –/+ Li in all groups). For the quantitative method, we used Total spectra with minimum value of 1 and normalization.

When the comparison is > 2 groups, one-way ANOVA test was used, otherwise t-test to identify the differential phosphoproteins with $p < 0.05$.

Somatic calcium imaging

Coverslips (12 mm) containing ~50,000 iPSC-derived neurons were washed with Krebs HEPES Buffer and incubated with 1 μM Fluo 4-AM (ThermoFisher F14201) in Krebs HEPES Buffer for 20 min at room temperature. Excess dye was removed by washing twice with Krebs HEPES Buffer, and cells were incubated for an additional 20 min to equilibrate the intracellular dye concentration and allow de-esterification. Then, cells were in Krebs HEPES buffer supplemented with the different drugs used for the Ca^{2+} experiment described in Fig. 4c. Live-cell imaging was performed by excitation of fluo 4 at 488 nm laser and measured at 520 nm at 25–26 °C on a field containing ~50 cells. 2 to 4 fields from a coverslip were imaged per line. A Time-lapse image sequences of 500 frames were acquired at ~2 Hz with a region of 512 pixels \times 512 pixels using a Andor digital camera (Andor solis). Images were subsequently processed using EZCalcium³¹ in Matlab software (MATLAB R2022b, MathWorks) to automatically identify the region of interest (ROI) which is the soma of the cells. Then, CaSiAn³¹ software implemented in Java was used to quantify the large Ca^{2+} events frequency in a semi-automated manner.

Immunoblot

Cells were homogenized in lysis buffer (10 mM Tris-HCl pH7.5, 10 mM EDTA, 150 mM NaCl, 1% Triton X100, 0.1% SDS) in the presence of a mammalian protease inhibitor cocktail (Sigma, P8340) and phosphoSTOP (Sigma 4906845001) to protect proteins from dephosphorylation. Protein extracts (30 μg) were resolved by SDS-PAGE, transferred onto PVDF membrane (Millipore IPFL00010), immunoblotted with the indicated concentration of primary antibodies: rabbit monoclonal anti-phospho-Akt (Thr308) (1/1000, Cell Signaling #4056, RRID: [AB_331163](#)), rabbit monoclonal anti-phospho-Akt (Ser 473) (1/1000; Cell Signaling #4060, RRID: [AB_2315049](#)); rabbit monoclonal anti-phospho-AMPK β 1 (Ser 108) (1/1000; Cell Signaling #23021); EIF4B phSer504 (1/1000; ThermoFisher #PA5114571). Standard GAPDH loading controls were included using a mouse monoclonal anti-GAPDH antibody (1/2000, ThermoFisher MAB5-15738). Then membrane was revealed using the appropriate LI-COR fluophore-conjugated secondary antibodies. Images were acquired on a LI-COR Odyssey Infrared image system. Fluorescence intensity values for each protein of interest were normalized to GAPDH signal from the same gel. Full-size blots for cropped gels can be found in extended data.

Drug treatment

The therapeutic range of Li treatment is between 0.75 and 1.5 mM. In this study, neurons were treated chronically with ~1.5 mM Li (Sigma L9650) for 7 days. Akt activator SC-79 (Tocris 4635) has been used in the literature^{32–34} between 5 and 10 μM . We chose to use low concentration (5 μM) but chronic treatment as Li treatment. A769662 (Sigma SML2578) is a potent activator of AMPK with half maximal effective concentration (EC50) of ~1 μM .³⁵ Thus, we used this concentration for our experiments. Based on the literature and several assays used previously, we used MAPK inhibitor U0126 (Tocris 1144) at 10 μM ^{36,37} and PKC inhibitor GF109203X (Tocris 0741) at 2 μM .³⁸ All the concentrations were chosen to activate or inhibit ~30–50% the kinase activity during 5–7 days.

Statistics

Statistical analyses were performed using GraphPad Prism 9 software (GraphPad software, Inc). All data are expressed as mean \pm standard error of the mean (s.e.m.). Normality for all groups was verified using the Shapiro-Wilk tests and $p < 0.05$ was considered significant. All statistical tests used are described in the figure legend.

Role of funders

The funding sources had no role in study design, collection of data analysis, and interpretation of data, in writing the report, or in the decision to submit the paper for publication.

Results

The composition of neuron cultures of Li-responsive and -non-responsive patients with BD is similar to those of controls

We sourced blood from patients with BD in well-characterized Li-responding and Li-non-responsive families, and age- and sex matched healthy individuals as controls (Ctl; no neuropsychiatric disease at the time of sample collection). These samples were used to isolate lymphocytes or peripheral blood mononuclear cells from which iPSCs were produced. Samples were selected based on clinical data according to the Alda scale for Li-responsiveness^{39,40} with a score of 9–10/10 for patients with BD who are Li-responsive (BD LR) and 0 to 3/10 for Li-non-responsive (BD LNR) (Table 1). All iPSCs lines were differentiated into neural progenitor cells (NPCs) with a minimum cut-off of ~90% of Nestin and Sox 2+ve cells (Supplementary Fig. S1a and b) for subsequent neuronal differentiation. At 4 weeks post-differentiation, neuronal phenotypes were confirmed by immunostaining for the neuron-specific marker beta-III tubulin/Tuj 1, which demonstrated ~75% of all cells were Tuj1+ve and therefore neuronal (Fig. 1a). Approximately 65% of all cells positive for Tuj1 were

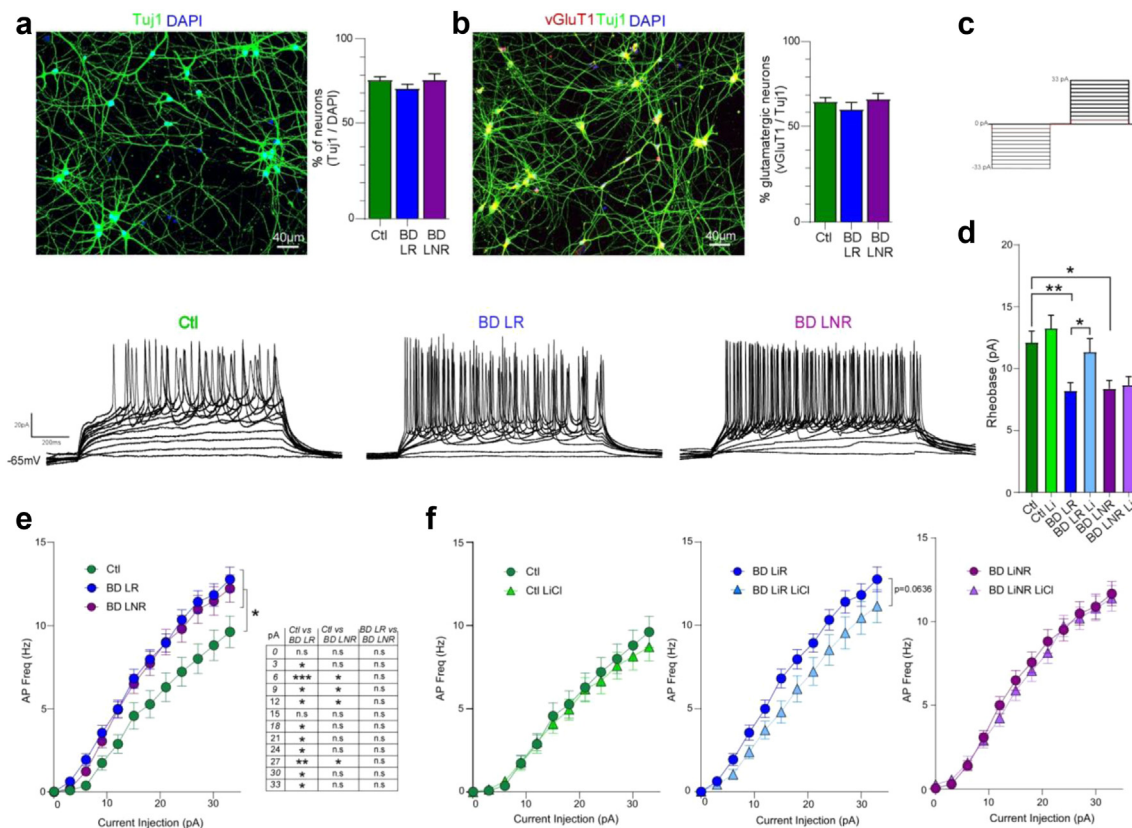


Fig. 1: Hyperexcitability in iPSC-derived neurons from patients with BD is selectively reversed by Li treatment in Li-responsive patient cell lines. **a–b)** Characterization of iPSC-derived neuron cultures at 4 weeks post-neuronal differentiation. **a)** cultures were stained for the neuronal marker (Tuj1) and nuclei (DAPI), in all lines. **b)** Glutamatergic neurons were identified by positive staining for the vesicular glutamate transporter (VGLUT1). **c)** Example of current-clamp membrane potential responses to 3 pA increasing positive and negative current injection steps from 0 to 33 pA (left) in Ctl, BD LR & BL LNR neurons. **d)** Mean neuronal rheobase was significantly lower in neurons from BD LR & LNR lines, relative to Ctl lines; Li significantly increased rheobase in BD LR neurons, but not BD LNR (or Ctl) neurons. **e–f)** Quantification of AP frequency (spikes/s) vs. positive current injection, and rheobase. **e)** BD (LR & LNR) neurons exhibit higher AP frequencies than Ctl neurons at all current steps above rheobase. **f)** Ctl, BD LR and LNR neurons ± Li (1.5 mM; 7d). Li had no effect on Ctl AP frequency plots, but reduced AP frequency in neurons from BD LR cell group. No differences in AP frequency plots were produced by Li in neurons from BD LNR lines. Data is percent + ve cells (mean ± SEM of each group, sampled from ~40 images fields in each of 4–5 lines per group) for (a–b), and mean ± SEM of ~50 neurons per condition from 4 to 5 different lines per group at 28–32 days post-neuronal differentiation (d–f). Statistical comparisons were by one-way (a, b & d) or two-way ANOVA (e–f) with Bonferroni’s multiple comparison post-test; *p < 0.05.

positive for the vesicular glutamate transporter 1(VGLUT1), indicating that majority of neurons are glutamatergic (Fig. 1b). There were no statistical differences in the cellular composition between Ctl and BD cultures. Immunostaining of cultures for non-neuronal glial-type cells showed very sparse labelling for the astrocytic marker GFAP, and none for the microglial marker iba 1 (Supplementary Fig. S4). Immunostaining results were corroborated by a computational deconvolution analysis of single cell reference data in RNA sequencing, demonstrating again that the cultures are almost entirely composed of cells with signatures corresponding to neurons or immature neuron/NPCs, with no differences in cellular composition between Ctl and BD cultures (Supplementary Fig. S4).

Neurons from patients with BD are hyperexcitable, and Li specifically reduces hyperexcitability in Li-responsive patient neurons

To assess the physiology of human neurones, we conducted whole-cell current-clamp recordings of neuronal intrinsic membrane properties and action potential (AP) characteristics. Current/Voltage (I/V) plot shows that membrane capacitance was significantly different in BD vs. Ctl neurons and upon Li treatment exclusively in BD LR neurons (see Supplementary Fig. S1i and j). Upon positive current injection, AP firing frequency was increased, and rheobase (amount of current needed to trigger an AP) was significantly reduced, in neurons from patients with BD relative to controls (Fig. 1c, d, e & f),

confirming the previous observation of hyperexcitability in both LR and LNR BD neurones.^{18,19} Chronic application of Li (1.5 mM for 7 days) resulted in significantly fewer APs for treatment effect in BD LR neurons and increased rheobase, specifically in BD neurones from LR patients; Li had no effect in Ctl or BD LNR neurons (Fig. 1d–f and Supplementary Fig. S1d and e).

In a subset of the same cells, we also conducted whole-cell voltage-clamp recording of spontaneous glutamatergic (holding voltage (V_h) –60 mV) and GABAergic (V_h at 0 mV) postsynaptic currents (sEPSCs and sIPSCs) respectively. We found a significant increase in sEPSC frequency in BD LR and LNR neurons, which was selectively reversed by Li treatment (1.5 mM, 7 days) in BD-LR neurons, but found no change to sIPSC frequency (Supplementary Fig. S2a–d).

Together, the data demonstrate intra-neuronal and excitatory network hyperactivity that is specifically reduced in only BD LR neurons by Li.

Increased Na⁺ current in neurons from LR patients with BD is rescued by Li

To further understand hyperexcitability in BD neurons we assayed Na⁺ and K⁺ currents by whole-cell

voltage clamp (Fig. 2a). We found a significant increase in Na⁺ current input/output curves, specifically in BD LR neurons, in concert with increased peak Na⁺ + conductance that trended to significance (Fig. 2b and c). There was a weaker trend to increased slow and fast K⁺ current flux in both BD LR and BD LNR, relative to controls (Fig. 2b–e). Li application resulted in a marked, significant, reduction of Na⁺ current input/output curves and peak conductance in BD LR neurons (Fig. 2f–g) but had no effect in BD LNR or Ctl neurons (Supplementary Fig. S3b–e). To ensure consistent Li effects within each patient line, we compare each separately and confirmed a significant reduction of Na⁺ current in neurons from each LR patient with BD (Supplementary Fig. S3a); whereas no reductions were observed in neurones from BD LNR or Ctl cell lines (Fig. 3c–e). While trends to altered fast and slow K⁺ currents in BD neurones did not reach significance, separate quantification of Li effects in each patient line showed a consistent and significant reduction of fast and slow K⁺ current exclusively in BD LR neurons (Supplementary Fig. S3g, i, k, l, o, q). The data demonstrate Na⁺ channel overactivation in BD LR neurons, and that Li treatment specifically reduces Na⁺ and K⁺ channel conductance in BD LR neurons.

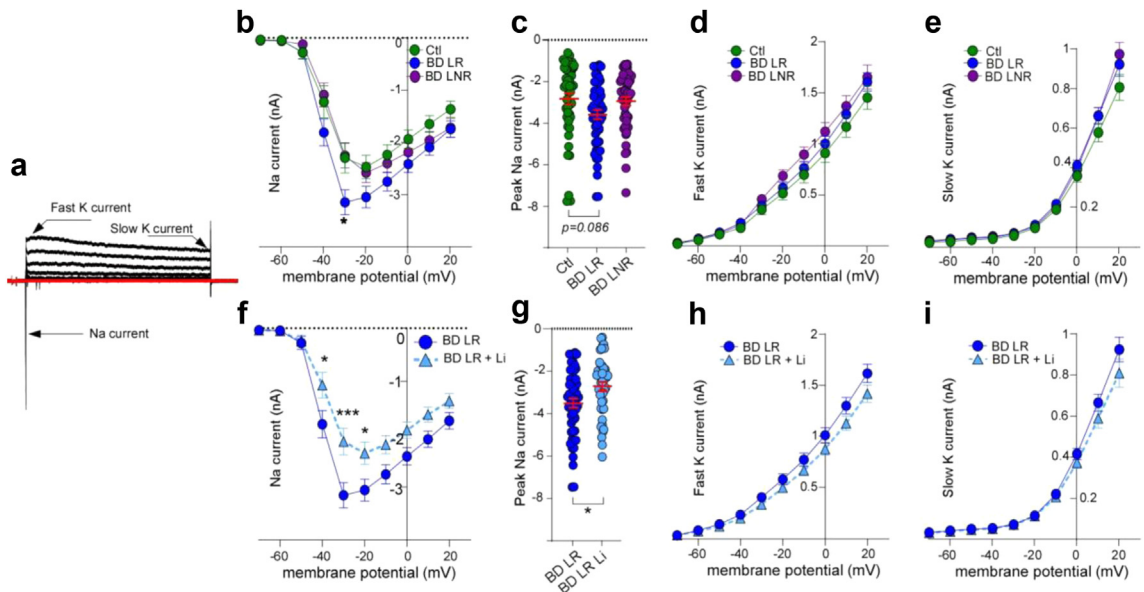


Fig. 2: Increased sodium current in neurons from LR patient lines with BD is normalised by Li. a) Example of voltage-clamp Na⁺ and K⁺ currents in response to 10 mV increasing positive voltage steps from –70 mV to 20 mV in Ctl neuron. Arrows indicate Na⁺ current and peak amplitude of fast and slow K⁺ currents. Quantification of voltage-dependence of b) peak sodium current vs. V_m c) maximum Na⁺ peak, d) fast and e) slow potassium current vs. V_m in Ctl, BD LR and BD LNR patient line neurons. f & g) Li (1.5 mM, 7d) reduced Na⁺ current peaks in BD LR neurons. h) Mean fast potassium and i) slow potassium current x voltage plots in BD LR neurons were reduced. Data are means ± SEM of ~50 neurons per condition from 4 to 5 different lines per group at 28–32 days post-neuronal differentiation. Statistical comparisons were by two-way (b, d, e, f, h, i) or one-way ANOVA (c-g) with Bonferroni’s multiple comparison post-test, and Welch’s t test was (d) ***p < 0.001, *p < 0.05.

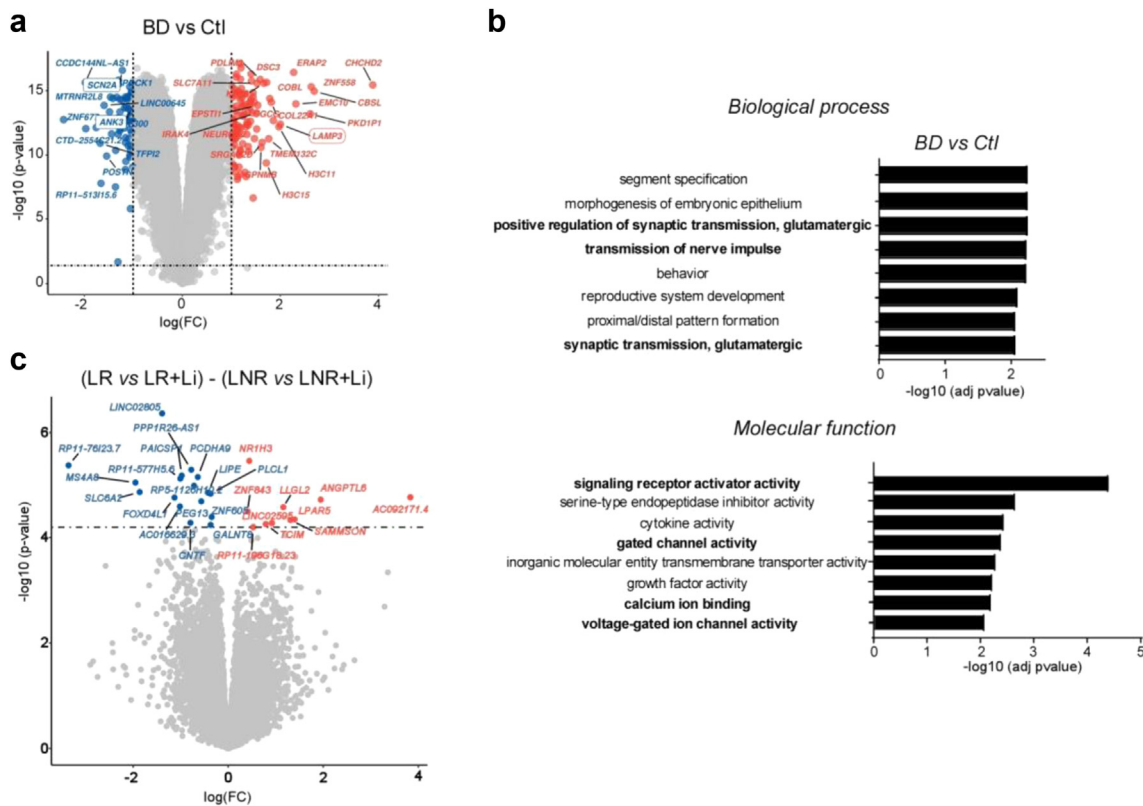


Fig. 3: Differential gene expression in neuronal cultures from patients with BD and identification of gene expression changes by Li application in LR and LNR patients with BD. **a**) Volcano plot shows Differential expressed genes (DEGs) in neurons from patients with BD vs. those from Ctl at ~30 days post-neuronal differentiation (data from 5 individual lines for Ctl and all 9 BD lines LR & LNR). DEGs were identified as those with an FDR corrected $p < 0.05$ and $\log FC > 1$. Framed genes are those previously identified by BD GWAS (see result section). **b**) Biological processes and molecular functions of DEG in BD neurons grouped by GO analysis, adjusted p value < 0.05 as threshold to define significant enriched pathways, which was corrected for multiple testing using FDR. **c**) Volcano plot shows difference in gene expression related to lithium in BD Li responders and non-responders. DEGs were identified as those with an FDR-corrected $p < 0.05$ and $\log FC > 1$.

Differential expression of ion transport & synaptic regulatory genes in BD neurons, and specific effects of Li on gene expression in LR & LNR neurons from patient with BD

To identify cellular processes underlying hyperexcitability in BD neurons, and effects of Li that are general or specific to BD LR neurons, we performed whole transcriptome sequencing from all patient lines. We compared neurons of Ctl vs. BD and LR $-/+$ Li vs LNR $-/+$ Li.

We identified 177 differential expressed genes (DEGs) in BD, relative to Ctl, in which 107 were up-regulated and 70 downregulated (Fig. 3a and Supplementary Table S1). Identified genes were noticeably involved in neuronal excitability, regulation of glutamatergic synapse function, neurotransmitter receptor and Ca^{2+} signalling, and ion transport/channel activity. Hits included GRIN2B, KCNJ6 and CACNG8 that encode for glutamate ionotropic receptor NMDA subunit 2B, K^+ inwardly rectifying channel subfamily J

member 6, and Ca^{2+} voltage gated channel auxiliary subunit 8, respectively. Of note, previously some identified hits in BD GWAS GWAS Catalog (ebi.ac.uk) were identified here as highly differentially expressed in BD neurons (Fig. 3a): SCN2A, ANK3, and LAMP3 which encode Na^+ voltage gated channel alpha subunit 2, Ankyrin 3, and lysosome associated protein 3.

Accordingly, gene ontology (GO) analysis for biological processes highlighted neuronal-specific transcripts, including those for glutamatergic transmission, as significantly altered in BD neurons, relative to Ctl. Similarly GO molecular function analysis suggested dysregulation of neurotransmitter receptor and Ca^{2+} signalling, in addition to ion channel activity (Fig. 3b).

The comparison of the different effect of Li in LR and LNR neurons identified 27 significant DEGs (Fig. 3c; Supplementary Table S2). There was no GO enrichment nor overlap with genes associated with lithium response in GWAS or with BD. However, the SLC6A2 (alias NET) was found; this gene encodes the

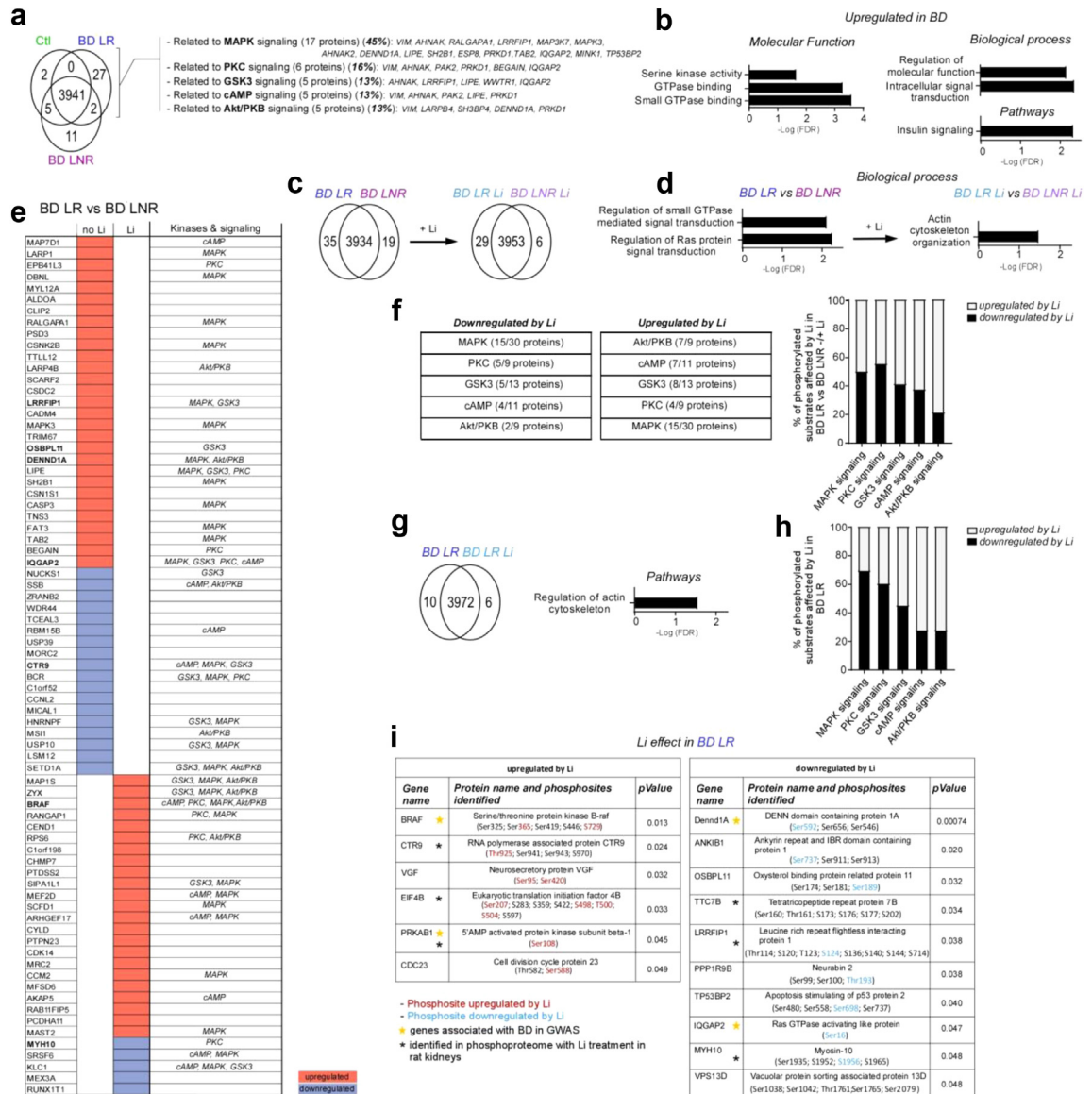


Fig. 4: Phosphoproteomic signature of BD and specific effects of Li in LR neurons. **a)** Venn diagram of phosphoproteins identified specific and common to Ctl, BD LR, and BD LNR neurons (left) and grouping of the BD-specific phosphoproteins listed by summary of their associated kinase/signaling cascades. **b)** Phosphoproteins unregulated in BD (vs. Ctl) grouped by molecular function and biological processes. **c)** Venn diagram of phosphoproteins common or specific to neurons from LR and LNR patient with BD in non-treated and Li conditions. **d)** Biological processes implicated in BD LR vs. BD LNR and by Li. **e)** Heat map shows differentially detected phosphoproteins in BD LR vs. BD LNR neurons between non- and Li-treated conditions. 47 differentially detected phosphoproteins are no longer present, and 28 phosphoproteins are newly detected, in Li treated BD LR vs. BD LNR neurons. Known kinases and signaling cascades for each identified phosphoprotein (substrate). Phosphoproteins linked to kinases also identified in BD LR +/- Li conditions are shown in bold. **f)** Table and summary graph showing the number and percentage of identified substrates (in E) that are phosphorylated by MAPK, PKC, GSK3, AMP and Akt signaling, and which is up or downregulated by Li treatment. **g)** Venn diagram showing differentially detected phosphoproteins in BD LR +/- Li, the pathways implicated, and **h)** the percentage of substrates regulated by MAPK, PKC, GSK3, AMP and Akt in non-vs Li-treated cells. **i)** Table listing the differentially detected phosphosites in the most significantly altered substrates identified from BD LR neurons +/- Li. Phosphosites highlighted in red or blue represent upregulated or downregulated phosphorylation by Li, respectively. Yellow star indicates association with BD in previous GWAS studies with "GWASdb SNP-Disease Associations" in harmonizome; black star highlights proteins regulated by Li identified in previous phosphoproteomics study (ref: <https://esbl.nhlbi.nih.gov/Databases/Lithium-Phospho-IMC/D/>). All data are from 4 lines per group/condition at ~30 days post-neuronal differentiation. Comparisons of >2 groups were conducted by one-way ANOVA, and separately by t-test for direct comparisons. Significance set at p < 0.05.

norepinephrine transporter and has been investigated in various psychiatric and addictive conditions.

It is important to note that RNA levels do not correlate well with proteins' levels or functional state. While DEGs highlight changes to potentially important processes, they do not inform on the molecular and biochemical status that might underlie molecular and physiological differences in BD, or the cell biological response to Li. That said, clear differences in the expression of genes related to neuronal and synaptic transmission were identified between Ctl and BD neurons.

Li promotes Akt signalling pathway activation in neurons from LR patients with BD

The activity of many kinases has been implicated in BD and Li effects,¹³ suggesting the phosphorylation state that governs both their activity, and that of their substrates, should form a consistent pattern. We therefore examined the phosphorylation profile of proteins to elucidate the signalling pathways altered in BD neurons, and which pathways respond to Li using unbiased label-free quantitative phosphoproteomics with nanoflow liquid chromatography tandem mass spectrometry (LC-MS/MS). Phosphopeptides, were enriched by titanium dioxide (TiO₂) in neuronal lysates from 4 patient lines per group to compare Ctl vs. BD, BD LR vs. BD LNR and BD LR vs. BD LNR $-/+$ Li.

We identified 6478, 7355 and 8559 phosphopeptides in Ctl, BD LR and BD LNR neurons, respectively (Supplementary Fig. S5a), belonging to ~4000 identified phosphoproteins. No change was observed in the overall percentage of phosphorylated serine, threonine, and tyrosine sites between groups, demonstrating no drastic change to global phosphorylation levels; ~85% of serine, ~14% of threonine, and ~1% of tyrosine residues were phosphorylated in all samples of Ctl, BD LR and BD LNR $-/+$ Li (Supplementary Fig. S5b). This finding is also a positive indicator of consistent sample preparation and quality control.

Statistical analyses identified 36, 15, and 43 proteins that were differentially phosphorylated between Ctl vs. BD LR, Ctl vs. BD LNR, and BD LR vs. BD LNR, respectively (Fig. 4a). Using a combination of bioinformatic resources and available proteomics database (phosphoSitePlus,⁴¹ Phospho. ELM,⁴² Networkin⁴³ and 'KEA substrates of kinase' & 'kinase library kinome Atlas' in Harmonizome⁴⁴) we determined which kinases are believed to phosphorylate the identified substrates, and group them to the pathways involved. We identified 5 main kinase signalling cascades: mitogen-activated protein kinase (MAPK), protein kinase C (PKC), glycogen synthase 3 (GSK3), protein kinase A (PKA) & AMP-activated protein kinase (AMPK) (both latter are strongly associated with intracellular adenosine monophosphate (AMP) levels) and protein kinase B (Akt) activity. Of the 27 proteins in the BD LR group with upregulated phosphorylation, we found 45% related to

MAPK signalling, and 16%, 13%, 13% and 13% related to PKC, GSK3, PKA&K and Akt signalling, respectively (Fig. 4a). Enrichment analysis (by g:profiler⁴⁵) also suggested an upregulation of small GTPase binding proteins in neurons from patients with BD, which are similarly involved in the regulation of intracellular signal transduction and insulin signalling (Fig. 4b). Interestingly, accumulating evidence suggest that disrupted insulin signalling is involved in bipolar disorder (BD) pathogenesis and/or mood stabilizer effects.^{5,46,47}

To isolate Li effects from beneficial neuronal (and clinical) Li-responsiveness, we compared BD LR vs. BD LNR $-/+$ Li, and BD LR vs. BD LR Li. We found that similarly to BD itself, Li affects small G-protein function and actin cytoskeleton organization. We identified 54 and 35 differentially phosphorylated proteins in BD LR vs. BD LNR and BD LR Li vs. BD LNR Li, respectively. There was an overlap of 7 proteins that were differentially phosphorylated in BD regardless of Li treatment (i.e. no effect of Li on the phosphorylation; Supplementary Fig. S5d). Then, 47 proteins were no longer detected as different in Li (i.e. phosphorylation differences reversed by Li; 18 upregulated and 29 downregulated by Li). Finally, 28 proteins that were only differentially phosphorylated in Li condition (i.e. phosphorylation altered by Li; 5 downregulated and 23 upregulated by Li; Fig. 4e). Linking the kinases that differentially phosphorylate the identified BD substrates reveal which signalling pathways are modulated by Li in neurons from LR patient with BD, and to what extent.

Each kinase/signalling cascaded we identified contains substrates that are downregulated and upregulated by Li, which seems to be paradoxical. Substrate phosphorylation is not only dictated by kinase activity, but also by many other determinants including other lower affinity kinases, cofactors, and subcellular localization/membrane associations. That said, the ratio between downregulation and upregulation of all substrates of a kinase or signalling pathway generally indicates the direction in which Li is altering the signalling pathway. Li appears to have moderate effects on downregulation of MAPK & PKC signalling and upregulation of PKA & AMPK signalling, alongside more profound effects on Akt signalling (Fig. 4f). A similar signalling profile (across 3972 phosphoproteins) was observed in BD LR vs. BD LR Li, with only 16 differentially phosphorylated proteins linked to the effects of Li (Fig. 4g and h). Of these 16 proteins, 6 were upregulated and 10 downregulated (Fig. 4g and Supplementary Fig. S5e, f, g). We validated upregulation of two phospho-sites by Li on two targets in BD LR neurons by Western blot, based on specificity of validated commercially available antibodies: PRKAB1 Ser 108 (AMPK β phSer108) and EIF4B phSer504 (Akt pathway) (Supplementary Fig. S5h and i). Of note, the specific phosphosites (Fig. 4i) we link here to Li's effect in LR patient neurons are consistent with

those implicated in previous BD GWAS (“GWASdb SNP-Disease Associations” in *harmonizome*) and Li phosphoproteomic studies (ref: <https://esbl.nhlbi.nih.gov/Databases/Lithium-Phospho-IMCD/>) (Fig. 4i).

Together, our phosphoproteomic results indicate that neurons from patient with BD exhibit upregulation of the small G-proteins that act as molecular switches to control several cellular processes including gene expression, cytoskeleton reorganization, vesicular transport, and intracellular signal transduction. Furthermore, the data argue that Li’s beneficial effects in neurons from LR patient with BD is through down-regulation of MAPK and PKC pathways, and upregulation of AMP and Akt pathways.

Akt activation phenocopies Li effects in neurons of LR patient with BD, and AMPK activation rescues elevated neural network activity and sodium conductance in neurons from LNR patient with BD

To test if the pathways we identified by phosphoproteomics can be modulated to mimic the positive effects of Li in neurons of LR patient with BD, we assessed the neural network activity following inhibition of MAPK (U0126), PKC (GF109203X), and activation of Akt (SC79), AMPK (A769662) signalling over the same time frame as Li application (5–7 days).

Neural network excitability was assayed by imaging activity-dependent somatic Ca^{2+} transients with Fluo 4-AM (Fig. 5a & b). Comparisons between Ctl, BD LR, and BD LNR in non-treated and drug conditions are displayed separately for clarity (Fig. 5c & d), but statistical testing is reported from comparison of all groups (Supplementary Fig. S6a). Compared to Ctl, LR and LNR neurons of patient with BD exhibited significantly higher Ca^{2+} event frequency (Fig. 5c), as predicted by hyperexcitability (Fig. 1e) and spontaneous sEPSC frequency (Supplementary Fig. S2) in neurons from patient with BD. In neurons from LR patient with BD, Li, Akt, and AMPK activators significantly reduced Ca^{2+} event frequency, whereas no change was observed with PKC or MAPK inhibition (Fig. 5d). This phenocopy suggests Li may act mainly via Akt and AMPK pathways to reduce neuronal activity and achieve its therapeutic effect in neurons from LR patient with BD. In neurons from LNR patient with BD, Li had no effect on the neural network activity (Fig. 5d), and MAPK inhibition increased event frequency (Fig. 5d). Interestingly, the activation of AMPK did reduce Ca^{2+} event frequency in neurons from LNR patient with BD, as was also observed in neurons from LR patient with BD (Fig. 5d). This suggest targeting AMPK activation could provide an alternative treatment for LR and LNR patients with BD.

To validate Akt and AMPK dysregulation in neurons from patient with BD, relative to Ctl, we quantified phosphorylation residues that report their activation state at Akt Thr308 & Ser 473, and AMPK Ser 108 by

Western blot (Fig. 5e & f). No changes were observed in Akt Thr308, whereas Akt Ser473 was hyperphosphorylated in neurons of LR patient with BD, and hypophosphorylated in BD LNR neurons, relative to Ctl (Fig. 5e and f). A differential phosphorylation of Akt Ser473 between BD LR and BD LNR groups may explain the opposite response in BD LR vs. BD LNR neurons to Li and Akt activation (Fig. 5c and d). Reduced AMPK Ser108 phosphorylation was found in neurons from patient with BD but was pronounced and statistically significant only in LNR neurons, relative to Ctl (Fig. 5e and f). This may explain why BD neurons were responsive to AMPK activation (Fig. 5d), whereas Ctl neurons were not (Supplementary Fig. S6A).

Together, network activity results confirm the predicted hyperactivity in neurons from patient with BD, and the selective rescue by Li only in LR neurons. Moreover, the data argue that Li acts via Akt pathway activation in neurons from LR patients with BD to trigger its therapeutic effect, and that this can be replicated in neurons from LR and LNR patient with BD by AMPK activation.

Finally, we sought to confirm that activators of Akt (SC79) and AMPK (A679662) have the predicted capacity to mimic Li effects on Na^+ and K^+ current in BD neurons. In BD LR neurons, the Akt activator (SC79) significantly reduced Na^+ and K^+ currents relative to non-treated neurons (Fig. 6a–e). The AMPK activator (A679662) decreased Na^+ current and K^+ in both BD groups (Fig. 6a–i) but peak Na^+ current reductions were significant only in BD LNR (Fig. 6f–i), suggesting that BD LNR neurons are more responsive to AMPK activation, as predicted by pronounced AMPK hypophosphorylation (Fig. 5f). Together the data confirm Akt & AMPK hypoactivity is linked to elevated Na^+ and K^+ conductance in neurons from patient with BD, and that pharmacological activation of Akt & AMPK can reduce neuronal hyperactivity in LR & LNR neurons from patients with BD.

Discussion

This study provides mechanistic insights into BD pathophysiology and Li’s mode of action, with direct clinical implications. Building from the observed physiological differences in BD neurons, and rescue of neural dysfunction as predicted by the patients’ clinical response to Li, we used transcriptomics and phosphoproteomics to define a molecular signature of BD, and the specific alterations induced by Li in responsive patient neurons. Focussing on kinase pathways implicated by ‘omics data, subsequent biochemical and pharmacological results argue that Akt and AMPK activation may serve as alternative treatment strategies to Li for BD.

While activation of Akt reversed network hyperactivity, and decreased Na^+ & K^+ currents in BD neurons

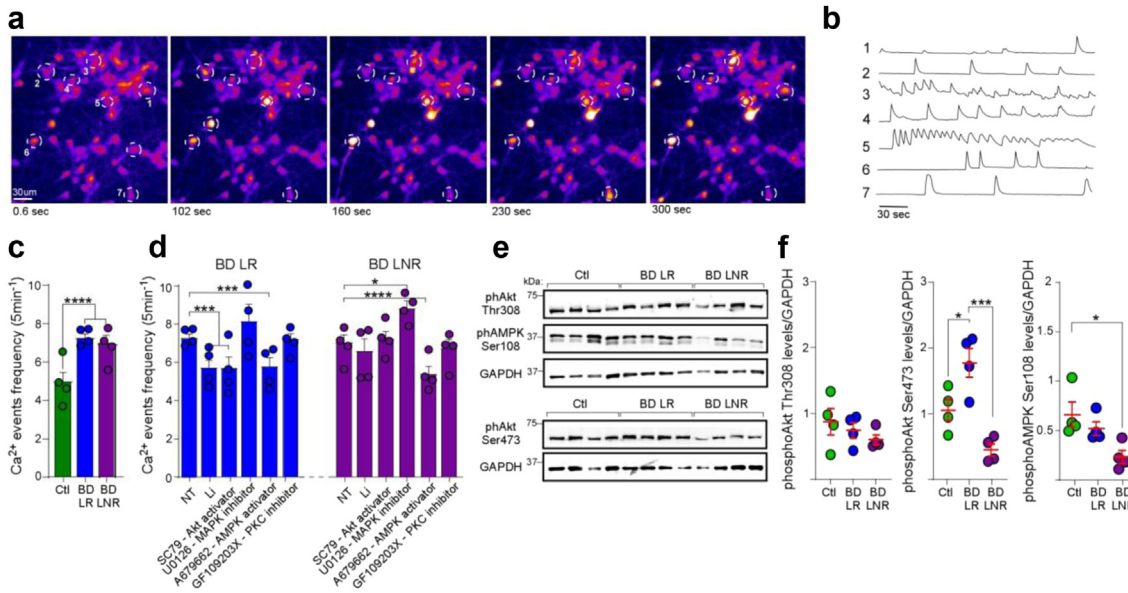


Fig. 5: Increased network activity in BD LR neurons is rescued by Akt & AMPK activation and only by AMPK activator in LNR neurons. *a*) Representative timelapse of Fluo 4 Ca^{2+} imaging of human neurons. *b*) Representative traces showing Ca^{2+} events (dF/F transients) from individual neurons (ROIs white dotted lines in *a*). *c*) Quantification of Ca^{2+} event frequency in neurons in non-treated (NT) condition Ctl & patient with BD. *d*) Quantification (within group) of NT neurons and those chronically (5–7 days) exposed to Li (1.5 mM), SC79-akt activator (5 μ M), U0126-MAPK inhibitor (10 μ M), A679662-AMPK activator (1 μ M), or GF109203X-PKC inhibitor (2 μ M). Data are mean \pm SEM of 4 lines per group/condition (500–800 cells per condition) at 30–35 days post-neuronal differentiation. Statistics: Two-way ANOVA with Bonferroni’s multiple comparisons test. * $p < 0.05$, *** $p < 0.001$, **** $p < 0.0001$. Representative immunoblots (*e*) and quantification (*f*) of phosphorylated Akt (Thr308) and (Ser 473), and AMPK β (Ser 108), normalized to GAPDH. Data shown means \pm SEM of 4 different lines per group at ~30 days post-neuronal differentiation. Statistics: one-way ANOVA with Bonferroni’s multiple comparison post-test *** $p < 0.001$, * $p < 0.05$.

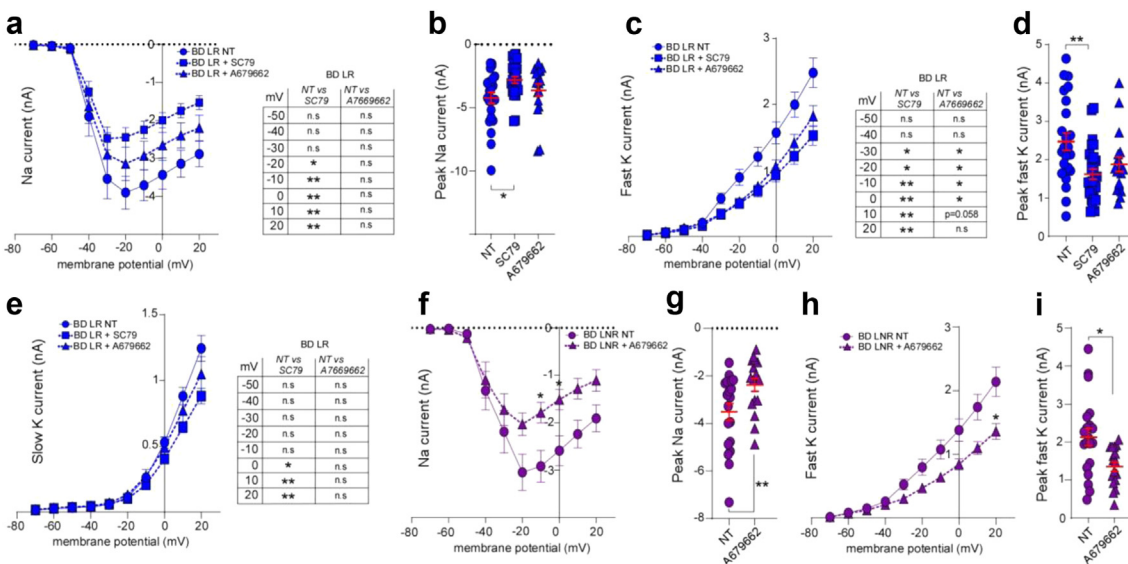


Fig. 6: Sodium and potassium currents are reduced by AMPK activator in LR and LNR neurons but only by Akt activator in LR neurons from patient with BD. Whole-cell voltage clamp recording of Na^+ (*a, b, f, g*) and K^+ (*c, d, e, h, i*) currents in LR & LNR neurons in non-treated (NT) or chronically applied SC79-akt activator (5 μ M) or A769662-AMPK activator (1 μ M). Data are mean \pm SEM of 20–27 neurons per condition, from 3 to 4 lines per group at 35–40 days post-neuronal differentiation. Statistics: Two-way ANOVA for *a, c, e, f, h* or one-way ANOVA for *b, d, g, i* with Bonferroni’s multiple comparisons test. ** $p < 0.01$, * $p < 0.05$.

from LR patients, AMPK activation reversed hyperactivity and decreased K currents in all BD neurons and Na currents in BD LNR neurons. The data suggests not only an alternative to Li for LR patients with BD, but also another approach for patients with BD who do not respond to Li.

We and others previously reported hyperexcitability in neurons of patients with BD,^{18–20} manifest as increased action potential firing and altered Na⁺ channel conductance. Here we confirm this and report the network/synaptic consequences of hyperexcitability in neurons from patients with BD, as evidenced by elevated activity-dependent Ca²⁺ bursts and increased spontaneous synaptic excitatory postsynaptic current frequency. A 7-day Li treatment reversed action potential, Na⁺ current, and Ca²⁺ burst hyperactivity in neurons from LR patients with BD; whereas neurons from LNR remained hyperactive. The therapeutic window for lithium is narrow (0.5~1.5 mM) and the line between efficacy and toxicity is fine. It is proposed that Li is toxic above 2 mM, both clinically and in iPSC-derived cortical neurons.^{48–50} We previously showed the chronic lithium treatment employed here, ~1.5 mM for 7 days, had no detectable toxicity in primary mouse cortical neurons,¹⁴ and we similarly found no cell death at this concentration in human neurons. Thus, we believe the effects of Li here are independent of toxicity, and therapeutically informative; furthermore, recapitulating Li effects with other less toxic kinase-modifying molecules may provide safer clinical tools.

A contemporary report in hiPSCs-derived cortical spheroids of patients with BD found right-shifted IV curves in response to current injection (indicative of decreased neuronal membrane excitability) at ~180 days post-differentiation, which was reversed by 30 days of exposure to Li.⁵¹ There were also fewer cells exhibiting spontaneous somatic Ca²⁺ signals in BD spheroids. However, the frequency of Ca²⁺ events was not different from controls, nor were any changes seen in Na channel peak conductance, action potentials, or sEPSC frequency in BD spheroids. Differences between the findings of Osete et al.⁵¹ and those here (and elsewhere^{18–20}) could be due to pronounced differences in the model systems, such as the density and maturity of neurons (both between studies, and between Ctl & BD spheroids).⁵¹ Regardless of such differences, the observation that sEPSC and Ca²⁺ burst frequencies in BD spheroids were similar to controls, despite much fewer BD cells being active, is suggestive of increased network activity in those neurons which are active in BD spheroids, consistent with the observations here. Alternatively, specific BD phenotypes might manifest at different stages of neuronal development/maturation, and it is possible a biphasic neuronal excitability phenotype exists in BD neurons, depending on maturity or the age of the preparation at the time of observation.

Our BD phosphoproteome analyses showed upregulation of small G-protein activity, which was rescued by Li in neurons from LR patient with BD. Small G-proteins modulate receptors and ion channel activity by influencing both channel open probability and channel trafficking to the plasma membrane.⁵² It is plausible that surface traffic and/or activity of neurotransmitter receptors, ion channels, and ion transporters would be dysregulated in BD LR neurons. Magnesium (Mg²⁺) is an essential cofactor for GTP-binding protein functions and is essential for guanine nucleotide binding and GTP-hydrolysis.⁵³ Li competes with Mg²⁺,⁵⁴ and thus could interfere with GTPase binding and activity. There is also known crosstalk between GTPases and Akt signalling pathways,^{55–57} which might explain why Akt activity is upregulated in BD LR and downregulated in BD LNR neurons (Fig. 5e and f). Further studies could directly assess GTPase activity in BD LR and LNR neurons and subsequent effects on neurotransmitter receptors, ion channel activity, and availability at the plasma membrane.

The phosphoproteomic data also show Li affected several kinases/pathways at different levels/degree, mainly activating Akt and AMPK in BD LR neurons, but also downregulating MAPK and PKC. All those changes could contribute to the observed physiological consequences, such as Li-dependent increases to rheobase, reduced Na⁺ currents, and Ca²⁺ events in BD LR neurons. The Akt activator (SC79) mimicked Li effects by reducing Na⁺ currents, and Ca²⁺ events in BD LR neurons, but also clearly reduced K⁺ channel conductance, which was only trending to being reduced by Li in BD LR neurons. This might indicate that activating Akt is more effective at reversing hyperactivity than Li. This also suggests that in Li treated BD LR neurons, K⁺ channel properties are not only regulated by Akt pathways. The AMPK activator (A-769662) reduced Ca²⁺ events, K⁺ currents, and to a lesser degree Na⁺ currents in BD LR neurons, which partially recapitulates the neurophysiological consequences of Li treatment. Together the data suggest Li mode of action results from the synergistic effects of several kinase pathways; however, both Akt and AMPK activators reduce hyperactivity (similarly to Li) in BD LR neurons, indicating potential clinical utility as alternative treatment strategies for patients with BD who are LR. The partially differential cellular responses to Li vs. Akt/AMPK activators could be explained by basal differences in Akt and AMPK activity we observed in untreated BD LR and BD LNR neurons. Phosphorylation of Akt Ser 473 was increased in BD LR neurons, and decreased in those of LNR patients with BD. The differential phosphorylation of Akt Ser473 could explain the differential responses to both Li and Akt activation in BD LR vs. LNR neurons. In support of this, growing evidence shows Akt-related kinases are implicated in schizophrenia and BD^{58–61}; specifically the activity of the Akt pathway is altered in the

forebrain of BD and schizophrenia subjects.⁵⁸ A recent report found Akt activation reduced peak Na⁺ current and neuronal excitability in rat cortical neurons,⁶² and others report that inhibition of Akt increased Na⁺ current and neuronal excitability in mouse CA1 hippocampal neurons.⁶³ Notably, Li activates Akt and this activation modulates mood-related behaviour in mice.⁶⁴ Together the literature and data here predict Akt activation may be therapeutically useful, but to our knowledge small molecule activators of Akt are yet to be tested in BD or other neuropsychiatric disorders.

We found phosphorylation of AMPK at Ser 108 was reduced in neurons from patients with BD, with a clearer difference in those from LNR patients. It is proposed that reduced AMPK activity contributes to the development of neuropsychiatric disorders and sleep disturbances.⁶⁵ Here, an AMPK activator reduced action potential hyperactivity, Na⁺, and K⁺-channel currents in BD LNR neurons. AMPK regulates Na⁺ and Ca²⁺ channels, and the Na/K pump^{66,67} responsible for maintaining neural membrane polarity and thus excitability. Activation of AMPK reduces excitability via inhibition of Na⁺ channels, regulates K⁺ channels leading to hyperpolarization, and dampens L-type Ca²⁺ channel currents.⁶⁶⁻⁶⁸ Here AMPK activation reduced neural activity in neurons from LR and LNR patients with BD; although reductions of Na⁺ and K⁺ current only reached statistical significance at 95% confidence in BD LNR neurons, suggesting they are more responsive to AMPK activation. A plausible explanation is our observation that AMPK activity was lower in BD LNR than BD LR neurons at base, making cellular effects of AMPK activation easier to detect. An alternative explanation, supported by a previous report,²⁰ is that hyperexcitability in BD LNR neurons is related to a reduction of Wnt/b-catenin signalling, and consequent downregulation of b-catenin/TCF/LEF1 transcriptional activity. The study of Santos et al.²⁰ showed Li had no effect on b-catenin in BD LNR cells, which had low b-catenin/TCF/LEF1 transcriptional activity. Thus, it is likely that Li could not reduce hyperexcitability in BD LNR through this pathway. Interestingly, b-catenin and its transcriptional activity are stabilized by AMPK phosphorylation of b-catenin at Ser 552⁶⁹; thus, crosstalk between Wnt/b-catenin and AMPK signalling could explain why AMPK activation dampened neural hyperactivity in BD LNR neurons.

It is of note that individuals with BD have a 2-fold increased risk of type II diabetes and insulin resistance is present in ~50% of patients with BD which might correlate with disease severity/progression.^{46,70,71} Recent reports suggested Li may exert its therapeutic effect in BD via insulin signalling.^{47,72} Akt and AMPK kinases are both also involved in insulin signalling and development of insulin resistance, and we found these to be dysregulated in BD neurons. A recent study found metformin (an AMPK activator) improved clinical

outcomes in patients with BD.⁷³ Specifically, in addition to decreased insulin resistance the patients who responded well to metformin reported improved mood disorder symptoms. This, and the results here support the use of AMPK activation for BD, and further confirmation studies are needed.

One of the limitations of this study is the use of neuronal monocultures, which do not reflect the complexity or function of the human brain, nor a whole organismal environment. While we demonstrate rescue of a neural phenotype by kinase activation, how this translates to a whole organism is yet to be determined. A lack of negative effects can be ascertained in animal models, but the neural hyperexcitability phenotype uncovered here in neurons from patient with BD has no animal model in which to validate a rescue effect. Another limitation is that 1.5 mM of Li is a high concentration in plasma and brain of patients with BD, that approaches toxic levels.⁴⁸⁻⁵⁰ The average Li concentration in whole brain and plasma of treated patients is ~1 mM; however, by ⁷Li magnetic resonance imaging in patients with BD treated for at least 2 years, Stout et al., showed heterogeneous distribution of Li in the brain, with some regions exposed to ~1.4 mM of Li. In this *in vitro* model, 1.5 mM of Li is not toxic for the neurons, but we do not rule out that this concentration of Li could have very different effects in a whole organism, including other organs such as the kidney or thyroid.

In summary, by utilizing hiPSC technology for personalized neuronal disease modelling, we found neuronal hyperactivity in neurons from patient with BD that was corrected by Akt and AMPK activators. We propose these as alternative treatment strategies for BD that require further preclinical testing. Future studies with larger samples and especially those including female patients, will be conducted to corroborate the results here, and help guide preclinical and clinical studies. This work also provides a framework for a personalized drug screening platform to accelerate development of other alternative therapeutic strategies for BD. Finally, this study demonstrates the capacity to distinguish between LR and LNR patient's neuronal response to Li (or other treatments) and predict a beneficial clinical response for individuals. This advances our capacity for personalized medicine in BD and could in future expedite the extreme lag between diagnosis and successful therapy selection, minimizing interim suffering and drastically reducing the risk of suicide.

Contributors

MA provided the patient samples. AK and YL developed the protocol for differentiation from iPSC to Neural Precursors then to forebrain neurons. YL grew and differentiated all the lines. AK performed the staining and imaging of neurons, analysed by AK and LS. AK, MAb and AKA performed the electrophysiological recordings. AK and MAb performed the Ca²⁺ imaging experiments. AK collected the RNA samples, CJ and QH analysed the RNA sequencing data. AK collected the protein

samples and KD performed phosphoenrichment, AK and KD analysed the phosphoproteomic data. AK collected protein samples and YC and AP performed the Western Blot. CEC and NF participated in methods development. AK and A.J.M contributed to study design, curation and development, and data interpretation. AK, G.A.R and A.J.M provided supervision and funding. AK, A.J.M, MA, and G.A.R have verified the underlying data. AK wrote the original draft edited by LS and A.J.M, which was revised and approved by all authors.

Data sharing statement

All relevant data are in the figures and supplementary figures. Any raw data and materials that can be shared will be released via a material transfer agreement. All transcriptomic data from this study are deposited in the GEO repository (GSE236482). Proteomic data could be made available upon requests directed to the corresponding author.

Declaration of interests

All the authors declare no conflict of interest.

Acknowledgements

We gratefully acknowledge the financial support of ERA PerMed (MA & G.A.R) #PLOT-BD, Bell Let's Talk-Brain Canada Mental Research Program (AM, MA, & G.A.R) #5450, and the Brain & Behavior Research Foundation Young investigator award (AK) #30822. We thank the microscopy platform of the Montreal Neurological Institute (MNI), and the Proteomics & Molecular Analysis Platform, RI-MUHC.

Appendix A. Supplementary data

Supplementary data related to this article can be found at <https://doi.org/10.1016/j.ebiom.2024.105161>.

References

- Vieta E, Berk M, Schulze TG, et al. Bipolar disorders. *Nat Rev Dis Prim*. 2018;4:18008.
- Moreira ALR, Van Meter A, Genzlinger J, Youngstrom EA. Review and meta-analysis of epidemiologic studies of adult bipolar disorder. *J Clin Psychiatry*. 2017;78(9):e1259–e1269.
- Kemp DE, Gao K, Chan PK, Ganocy SJ, Findling RL, Calabrese JR. Medical comorbidity in bipolar disorder: relationship between illnesses of the endocrine/metabolic system and treatment outcome. *Bipolar Disord*. 2010;12(4):404–413.
- Forty L, Ulanova A, Jones L, et al. Comorbid medical illness in bipolar disorder. *Br J Psychiatry*. 2014;205(6):465–472.
- Coello K, Vinberg M, Knop FK, et al. Metabolic profile in patients with newly diagnosed bipolar disorder and their unaffected first-degree relatives. *Int J Behav Dev*. 2019;7(1):8.
- Kerner B. Genetics of bipolar disorder. *Appl Clin Genet*. 2014;7:33–42.
- Kerner B. Toward a deeper understanding of the genetics of bipolar disorder. *Front Psychiatr*. 2015;6:105.
- Craddock N, Sklar P. Genetics of bipolar disorder. *Lancet (London, England)*. 2013;381(9878):1654–1662.
- Mullins N, Forstner AJ, O'Connell KS, et al. Genome-wide association study of more than 40,000 bipolar disorder cases provides new insights into the underlying biology. *Nat Genet*. 2021;53(6):817–829.
- Cipriani A, Hawton K, Stockton S, Geddes JR. Lithium in the prevention of suicide in mood disorders: updated systematic review and meta-analysis. *BMJ*. 2013;346:f3646.
- Alda M. Lithium in the treatment of bipolar disorder: pharmacology and pharmacogenetics. *Mol Psychiatr*. 2015;20(6):661–670.
- Alda M. Who are excellent lithium responders and why do they matter? *World Psychiatr*. 2017;16(3):319–320.
- Khayachi A, Schorova L, Alda M, Rouleau GA, Milnerwood AJ. Posttranslational modifications & lithium's therapeutic effect—potential biomarkers for clinical responses in psychiatric & neurodegenerative disorders. *Neurosci Biobehav Rev*. 2021;127:424–445.
- Khayachi A, Ase A, Liao C, et al. Chronic lithium treatment alters the excitatory/inhibitory balance of synaptic networks and reduces mGluR5-PCK signalling in mouse cortical neurons. *J Psychiatry Neurosci*. 2021;46(3):E402–E414.
- Saxena A, Scaini G, Bavaresco DV, et al. Role of protein kinase C in bipolar disorder: a review of the current literature. *Mol Neuropsychiatry*. 2017;3(2):108–124.
- Hahn CG, Umapathy Wang HY, Koneru R, Levinson DF, Friedman E. Lithium and valproic acid treatments reduce PKC activation and receptor-G protein coupling in platelets of bipolar manic patients. *J Psychiatr Res*. 2005;39(4):355–363.
- Noble W, Planel E, Zehr C, et al. Inhibition of glycogen synthase kinase-3 by lithium correlates with reduced tauopathy and degeneration *in vivo*. 2005;102(19):6990–6995.
- Mertens J, Wang QW, Kim Y, et al. Differential responses to lithium in hyperexcitable neurons from patients with bipolar disorder. *Nature*. 2015;527(7576):95–99.
- Stern S, Santos R, Marchetto MC, et al. Neurons derived from patients with bipolar disorder divide into intrinsically different subpopulations of neurons, predicting the patients' responsiveness to lithium. *Mol Psychiatr*. 2018;23(6):1453–1465.
- Santos R, Linker SB, Stern S, et al. Deficient LEF1 expression is associated with lithium resistance and hyperexcitability in neurons derived from bipolar disorder patients. *Mol Psychiatr*. 2021;26(6):2440–2456.
- Milnerwood AJ, Kaufman AM, Sepers MD, et al. Mitigation of augmented extrasynaptic NMDAR signaling and apoptosis in cortico-striatal co-cultures from Huntington's disease mice. *Neurobiol Dis*. 2012;48(1):40–51.
- Brigidi GS, Sun Y, Beccano-Kelly D, et al. Palmitoylation of delta-catenin by DHH5 mediates activity-induced synapse plasticity. *Nat Neurosci*. 2014;17(4):522–532.
- Dobin A, Davis CA, Schlesinger F, et al. STAR: ultrafast universal RNA-seq aligner. *Bioinformatics*. 2013;29(1):15–21.
- Li B, Dewey CN. RSEM: accurate transcript quantification from RNA-Seq data with or without a reference genome. *BMC Bioinf*. 2011;12(1):323.
- Robinson MD, McCarthy DJ, Smyth GK. edgeR: a Bioconductor package for differential expression analysis of digital gene expression data. *Bioinformatics*. 2010;26(1):139–140.
- Langfelder P, Horvath S. WGCNA: an R package for weighted correlation network analysis. *BMC Bioinf*. 2008;9(1):559.
- Ritchie ME, Phipson B, Wu D, et al. Limma powers differential expression analyses for RNA-sequencing and microarray studies. *Nucleic Acids Res*. 2015;43(7):e47–e.
- Leek JT. svaseq: removing batch effects and other unwanted noise from sequencing data. *Nucleic Acids Res*. 2014;42(21):e161–e.
- Yu G, Wang LG, Han Y, He QY. clusterProfiler: an R package for comparing biological themes among gene clusters. *OMICS*. 2012;16(5):284–287.
- Sutton GJ, Poppe D, Simmons RK, et al. Comprehensive evaluation of deconvolution methods for human brain gene expression. *Nat Commun*. 2022;13(1):1358.
- Cantu DA, Wang B, Gongwer MW, et al. EZcalcium: open-source toolbox for analysis of calcium imaging data. *Front Neural Circ*. 2020;14:25.
- Jo H, Mondal S, Tan D, et al. Small molecule-induced cytosolic activation of protein kinase Akt rescues ischemia-elicited neuronal death. *Proc Natl Acad Sci U S A*. 2012;109(26):10581–10586.
- So EY, Ouchi T. BRAT1 deficiency causes increased glucose metabolism and mitochondrial malfunction. *BMC Cancer*. 2014;14:548.
- Zhang B, Wang W, Li C, Liu R. Inositol polyphosphate-4-phosphatase type II plays critical roles in the modulation of cadherin-mediated adhesion dynamics of pancreatic ductal adenocarcinomas. *Cell Adhes Migrat*. 2018;12(6):548–563.
- Cool B, Zinker B, Chiu W, et al. Identification and characterization of a small molecule AMPK activator that treats key components of type 2 diabetes and the metabolic syndrome. *Cell Metabol*. 2006;3(6):403–416.
- Eppstein AC, Sandoval JA, Klein PJ, et al. Differential sensitivity of chemoresistant neuroblastoma subtypes to MAPK-targeted treatment correlates with ERK, p53 expression, and signaling response to U0126. *J Pediatr Surg*. 2006;41(1):252–259.
- Freeman MR, Kim J, Lisanti MP, Di Vizio D. A metabolic perturbation by U0126 identifies a role for glutamine in resveratrol-induced cell death. *Cancer Biol Ther*. 2011;12(11):966–977.
- Finan GM, Realubit R, Chung S, et al. Bioactive compound screen for pharmacological enhancers of apolipoprotein E in primary human astrocytes. *Cell Chem Biol*. 2016;23(12):1526–1538.
- Nunes A, Trappenberg T, Alda M, The international Consortium on Lithium G. Asymmetrical reliability of the Alda score favours a

- dichotomous representation of lithium responsiveness. *PLoS One*. 2020;15(1):e0225353.
- 40 Manchia M, Adli M, Akula N, et al. Assessment of response to lithium maintenance treatment in bipolar disorder: a consortium on lithium genetics (ConLiGen) report. *PLoS One*. 2013;8(6):e65636.
 - 41 Hornbeck PV, Kornhauser JM, Tkachev S, et al. PhosphoSitePlus: a comprehensive resource for investigating the structure and function of experimentally determined post-translational modifications in man and mouse. *Nucleic Acids Res*. 2012;40(Database issue):D261–D270.
 - 42 Dinkel H, Chica C, Via A, et al. Phospho.ELM: a database of phosphorylation sites—update 2011. *Nucleic Acids Res*. 2011;39(Database issue):D695–D699.
 - 43 Linding R, Jensen LJ, Pasculescu A, et al. NetworKIN: a resource for exploring cellular phosphorylation networks. *Nucleic Acids Res*. 2008;36(Database issue):D695–D699.
 - 44 Rouillard AD, Gundersen GW, Fernandez NF, et al. The harmonizome: a collection of processed datasets gathered to serve and mine knowledge about genes and proteins. *Database*. 2016;2016.
 - 45 Raudvere U, Kolberg L, Kuzmin I, et al. g:Profiler: a web server for functional enrichment analysis and conversions of gene lists (2019 update). *Nucleic Acids Res*. 2019;47(W1):W191–W198.
 - 46 Calkin CV, Ruzickova M, Uher R, et al. Insulin resistance and outcome in bipolar disorder. *Br J Psychiatr*. 2015;206(1):52–57.
 - 47 Campbell IH, Campbell H, Smith DJ. Insulin signaling as a therapeutic mechanism of lithium in bipolar disorder. *Transl Psychiatry*. 2022;12(1):350.
 - 48 Izsak J, Seth H, Iljin M, et al. Differential acute impact of therapeutically effective and overdose concentrations of lithium on human neuronal single cell and network function. *Transl Psychiatry*. 2021;11(1):281.
 - 49 Gitlin M. Lithium side effects and toxicity: prevalence and management strategies. *Int J Bipolar Disord*. 2016;4(1):27.
 - 50 Hedy SA, Avula A, Swoboda HD. *Lithium toxicity*. StatPearls. Treasure Island (FL): StatPearls publishing copyright © 2024. StatPearls Publishing LLC.; 2024.
 - 51 Osete JR, Akkouch IA, Ievglevskiy O, et al. Transcriptional and functional effects of lithium in bipolar disorder iPSC-derived cortical spheroids. *Mol Psychiatr*. 2023;28:3033.
 - 52 Pochynyuk O, Stockand JD, Staruschenko A. Ion Channel regulation by ras, Rho, and Rab. *Small GTPases*. 2007;232(10):1258–1265.
 - 53 Zhang B, Zhang Y, Wang Z, Zheng Y. The role of Mg²⁺ cofactor in the guanine nucleotide exchange and GTP hydrolysis reactions of Rho family GTP-binding proteins. *J Biol Chem*. 2000;275(33):25299–25307.
 - 54 Srinivasan C, Toon J, Amari L, et al. Competition between lithium and magnesium ions for the G-protein transducin in the guanosine 5'-diphosphate bound conformation. *J Inorg Biochem*. 2004;98(5):691–701.
 - 55 Ahn JY, Rong R, Kroll TG, Van Meir EG, Snyder SH, Ye K. PIKE (phosphatidylinositol 3-kinase enhancer)-A GTPase stimulates Akt activity and mediates cellular invasion. *J Biol Chem*. 2004;279(16):16441–16451.
 - 56 Genot EM, Arriemerlou C, Ku G, Burgering BMT, Weiss A, Kramer IM. The T-cell receptor regulates akt (protein kinase B) via a pathway involving Rac 1 and Phosphatidylinositide 3-kinase. *Mol Cell Biol*. 2000;20(15):5469–5478.
 - 57 Sugden PH. Ras, Akt, and mechanotransduction in the cardiac myocyte. 2003;93(12):1179–1192.
 - 58 Vanderplow AM, Eagle AL, Kermath BA, Bjornson KJ, Robison AJ, Cahill ME. Akt-mTOR hypoactivity in bipolar disorder gives rise to cognitive impairments associated with altered neuronal structure and function. *Neuron*. 2021;109(9):1479–1496.e6.
 - 59 Campbell I, Campbell H. Mechanisms of insulin resistance, mitochondrial dysfunction and the action of the ketogenic diet in bipolar disorder. Focus on the PI3K/AKT/HIF1- α pathway. *Med Hypotheses*. 2020;145:110299.
 - 60 Wong H, Levenga J, LaPlante L, et al. Isoform-specific roles for AKT in affective behavior, spatial memory, and extinction related to psychiatric disorders. *Elife*. 2020;9:e56630.
 - 61 Tsimberidou A-M, Skliris A, Valentine A, et al. AKT inhibition in the central nervous system induces signaling defects resulting in psychiatric symptomatology. *Cell Biosci*. 2022;12(1):56.
 - 62 Arribas-Blázquez M, Piniella D, Olivos-Oré IA, et al. Regulation of the voltage-dependent sodium channel Na(V)1.1 by AKT1. *Neuropharmacology*. 2021;197:108745.
 - 63 Marosi M, Nenov MN, Di Re J, Dvorak NM, Alshammari M, Laezza F. Inhibition of the akt/PKB kinase increases Nav 1.6-Mediated Currents and Neuronal Excitability in CA1 Hippocampal Pyramidal Neurons. *Int J Mol Sci*. 2022;23(3):1700.
 - 64 Pan JQ, Lewis MC, Ketterman JK, et al. AKT kinase activity is required for lithium to modulate mood-related behaviors in mice. *Neuropsychopharmacology*. 2011;36(7):1397–1411.
 - 65 Nagy S, Maurer GW, Hentze JL, Rose M, Werge TM, Rewitz K. AMPK signaling linked to the schizophrenia-associated 1q21.1 deletion is required for neuronal and sleep maintenance. *PLoS Genet*. 2018;14(12):e1007623.
 - 66 Lang F, Föller M. Regulation of ion channels and transporters by AMP-activated kinase (AMPK). *Channels*. 2014;8(1):20–28.
 - 67 Andersen MN, Rasmussen HB. AMPK: a regulator of ion channels. *Commun Integr Biol*. 2012;5(5):480–484.
 - 68 Bermeo K, Castro H, Arenas I, Garcia DE. AMPK mediates regulation of voltage-gated calcium channels by leptin in isolated neurons from arcuate nucleus. 2020;319(6):E1112–E1120.
 - 69 Zhao J, Yue W, Zhu MJ, Sreejayan N, Du M. AMP-activated protein kinase (AMPK) cross-talks with canonical Wnt signaling via phosphorylation of β -catenin at Ser 552. *Biochem Biophys Res Commun*. 2010;395(1):146–151.
 - 70 Coello K, Vinberg M, Knop FK, et al. Metabolic profile in patients with newly diagnosed bipolar disorder and their unaffected first-degree relatives. *Int J Bipolar Disord*. 2019;7(1):8.
 - 71 Calkin CV. Insulin resistance takes center stage: a new paradigm in the progression of bipolar disorder. *Ann Med*. 2019;51(5–6):281–293.
 - 72 Tye SJ, Borreggine K, Price JB, et al. Dynamic insulin-stimulated mTOR/GSK3 signaling in peripheral immune cells: preliminary evidence for an association with lithium response in bipolar disorder. *Bipolar Disord*. 2022;24(1):39–47.
 - 73 Calkin CV, Chengappa KNR, Cairns K, et al. Treating insulin resistance with metformin as a strategy to improve clinical outcomes in treatment-resistant bipolar depression (the TRIO-BD study): a randomized, quadruple-masked, placebo-controlled clinical trial. *J Clin Psychiatry*. 2022;83(2).